IOPscience iopscience.iop.org

Home Search Collections Journals About Contact us My IOPscience

Stopping power of semiconducting III-V compounds for low-energy electrons

This content has been downloaded from IOPscience. Please scroll down to see the full text.

1986 J. Phys. D: Appl. Phys. 19 255

(http://iopscience.iop.org/0022-3727/19/2/012)

View the table of contents for this issue, or go to the journal homepage for more

Download details:

IP Address: 140.113.38.11
This content was downloaded on 28/04/2014 at 20:42

Please note that terms and conditions apply.

J. Phys. D: Appl. Phys. 19 (1986) 255–263. Printed in Great Britain

Stopping power of semiconducting III–V compounds for low-energy electrons†

C M Kwei‡ and C J Tung§
‡ Department of Electronics Engineering, National Chiao Tung University, Hsinchu, Taiwan 300, China
§ Institute of Nuclear Science, National Tsing Hua University, Hsinchu, Taiwan 300, China

Received 18 April 1985

Abstract. The stopping power of III–V compounds for incident electrons has been studied. An extended Drude-type dielectric function has been employed for the response of valence band. The local plasma approximation has been applied for the response of inner shells. Stopping powers of GaAs, GaSb, GaP, InSb, and InAs were computed and compared to the limited data.

1. Introduction

Stopping power is an important parameter for the study of charged particle transport properties (see e.g. Berger and Seltzer 1982). Computation of this quantity requires a description about the response of the media to the external probes. In the case of condensed matter, this response may be separated into the contribution from the valence band and inner shells (Fano 1963). A bulk response function described by the dissipative part of the dielectric function is applied to the valence band. Alternatively, the atomic response function associated with the excitation of a given inner shell is employed for inner shells.

In this paper we have studied the stopping power of semiconducting III–V compounds for incident electrons of low energy (<10 keV). This study finds its application (Willardson and Beer 1967) in Auger electron spectroscopy, x-ray photoelectron spectroscopy, surface physics, microdosimetry, etc. Very little work has been done with respect to such study in the important media of semiconducting III–V compounds. Part of the reason from the theoretical point of view is the difficulty involved in treating the large number of inner shells (Tung *et al* 1979). The stopping power for high-energy electrons is relatively easy to compute using the Bethe theory (Berger and Seltzer 1982).

The successful application of the local plasma approximation (LPA) to estimate the mean excitation energy of gaseous (Chou and Powers 1972) and condensed (Ziegler 1980) matter suggests that the same procedures assumed by the approximation may be applicable to the stopping powers contributed by inner shells. This approximation is expected to work poorly for the stopping power contributed by the valence band because of the strong correlation of electrons in the band leading to a large damping effect in

† Research sponsored by the National Science Council of the Republic of China.

contrast with the assumption. In this work we adopt an approach which involves the dielectric function for the valence band and local plasma approximation for inner shells.

Although accurate calculation of the dielectric function should be based on realistic band structures and wavefunctions, a model calculation is often quite useful in studying the electro-optical properties of the stopping medium. Here we use a model based on the Drude-type model but generalised to make it compatible with the response characterised by the dielectric functions of III–V compound semiconductors. We started with an expression for the imaginary part of a long-wavelength dielectric function. The real part of the function and consequently the energy loss function were set up by means of the Kramers–Kronig analysis. Corresponding quantities at any wavelengths have been generalised by a simple relation which worked within first-order accuracy of the squared wave-vectors.

For inner shells, the application of the LPA was incorporated with the electron density distributions computed by the Hartree–Slater model (Herman and Skillman 1963). Previous study on the various moments of the oscillator strength distribution proved that such an approach was valid for the broad region of excitation energy for inner shell electrons (Tung and Watt 1985).

2. Valence band

The response of the valence band to the external probe may be described by the complex dielectric function. The real and imaginary parts of this function contain information which reflects the band structure and the characteristic energy losses associated with the transition of electrons in the band. In the case of semiconducting III–V compounds, the imaginary part of the dielectric function displays double peaks which correspond to the excitation of valence electrons to the conduction band. Other faint humps corresponding to the interband transitions of weakly deep-lying levels are superimposed on to the main peaks.

In this work, we consider the general case that the valence band is formed by several groups of electrons, each group with its distinct oscillator strength, eigenfrequency, and damping constant. The imaginary part of the dielectric function in the long-wavelength limit is given by (Tung and Lin 1984)

$$\varepsilon_2(0, \omega) = \sum_i \frac{A_i \gamma_i \omega}{(\omega^2 - \omega_i^2)^2 + \omega^2 \gamma_i^2} \tag{1}$$

where A_i, γ_i, and ω_i are, respectively, the oscillator strength, damping constant, and eigenfrequency associated with the ith group of electrons in the III–V compounds. The real part of the dielectric function is obtained using the Kramers–Kronig relation. The result is

$$\varepsilon_1(0, \omega) = 1 - \sum_i \frac{A_i(\omega^2 - \omega_i^2)}{(\omega^2 - \omega_i^2)^2 + \omega^2 \gamma_i^2}. \tag{2}$$

The energy loss function, i.e. the imaginary part of the negative reciprocal dielectric function, is then determined by

$$\operatorname{Im}\left(-\frac{1}{\varepsilon(0, \omega)}\right) = \frac{\varepsilon_2}{\varepsilon_1^2 + \varepsilon_2^2}. \tag{3}$$

To determine A_i, γ_i, and ω_i, we first fit ε_2 in equation (1) to the values computed from energy loss measurements. We require also that the calculated ε_1 and $\mathrm{Im}(-1/\varepsilon)$ from (2) and (3) are in good agreement with the experimental results. Furthermore, the total oscillator strength as determined by a sum of A_i over all available sub-bands must satisfy the sum rule

$$\sum_i A_i = \omega_{\mathrm{pv}}^2 = 4\pi n_{\mathrm{v}} \tag{4}$$

where ω_{pv} and n_{v} are the plasma frequency and density of valence electrons. Note that we use atomic units (au) for all quantities and expressions in this paper.

To extrapolate the dielectric function into the $k \neq 0$ region of the k–ω plane, where k is the wave-vector, we let $\omega_i \rightarrow \omega_i(k) = \omega_i + k^2/2$. This relation works correctly at the two ends of the k region, i.e. $k \rightarrow 0$ and $k \rightarrow \infty$. As pointed out by Ritchie *et al* (1975), the Bethe ridge, a region in the neighbourhood of the free-electron line $\omega = k^2/2$, is the asymptotic limit of the energy–momentum relation at $k \rightarrow \infty$. The limit of $\omega_i(k)$ in the optical end approaches to the eigenfrequency ω_i of the ith sub-band, each making its own more-or-less distinct contribution to the dielectric function. The assumed relation $\omega_i(k)$ works within first-order accuracy of k^2.

The contribution of the valence band to the stopping power for electrons is obtained by (Tung and Ritchie 1977)

$$S_{\mathrm{v}}(E) = \frac{1}{\pi E} \int_0^E \omega \, \mathrm{d}\omega \int_{k_-}^{k_+} \frac{\mathrm{d}k}{k} \mathrm{Im}\left(-\frac{1}{\varepsilon(k, \omega)}\right) \tag{5}$$

where $k_\pm = \sqrt{2E} \pm \sqrt{2E - 2\omega}$ and E is the energy of the incident electron.

3. Inner shells

For the well localised inner shells, the bulk response described by the dielectric function breaks down to a collection of the individual responses of each atom. These responses are characterised by the generalised oscillator strength (GOS) which relates to the energy loss function by (Fano 1963)

$$\frac{\mathrm{d}f_i}{\mathrm{d}\omega} = \frac{\omega}{2\pi^2} \mathrm{Im}\left(-\frac{1}{\varepsilon(k, \omega)}\right) \tag{6}$$

where $\mathrm{d}f_i/\mathrm{d}\omega$ is the GOS per atom associated with the ith inner shell.

The local plasma approximation developed by Lindhard and Scharff (1953) and applied to estimate the mean excitation energy for many materials, takes the following procedures. First, let $\gamma \rightarrow 0$ and $\omega_{\mathrm{p}}^2 \rightarrow \omega_{\mathrm{p}}^2(r) = 4\pi n(r)$ in the concerned quantity involving the dielectric function. Then average the quantity by weighting it with the electron density distribution, $4\pi r^2 n(r)$ of the atom. Applying the first procedure to the dielectric function (Raether 1980)

$$\varepsilon(0, \omega) = 1 + \sum_i \frac{\omega_{pi}^2}{\omega_i^2 - \omega^2 + i\gamma\omega} \tag{7}$$

and equation (6) for inner shells, we obtain

$$\frac{df_i}{d\omega} = \frac{\omega z_i}{\tilde{\omega}_p + k^2/2}[\omega - (\tilde{\omega}_p + k^2/2)] \tag{8}$$

where z_i is the number of electrons per atom in the ith inner shell and ω_{pi} is the plasma frequency of the ith inner shell electrons as if they were free. Here again we have extended the dielectric function to the $k \neq 0$ region by the process described previously. The altered plasma frequency of bound electrons is determined by

$$\prod_i (\omega_i^2 - \tilde{\omega}_p^2) + \sum_i \left\{\omega_{pi}^2 \left[\prod_{j\neq i} (\omega_j^2 - \tilde{\omega}_p^2)\right]\right\} = 0. \tag{9}$$

For simplicity, we assume that the contribution of each inner shell to the dielectric function of equation (7) can be separately evaluated. This assumption is approximately correct for inner shells which are well separated in regard to their binding energies. Taking a single inner shell to equation (7), equation (8) remains the same and (9) becomes

$$\tilde{\omega}_p = (\omega_{pi}^2 + \omega_i^2)^{1/2}. \tag{10}$$

Substituting (6) and (8) into (5), we find the contribution of ith inner shell to the stopping power to be

$$S_i(E) = \frac{2\pi N_i}{E} \ln \frac{\sqrt{E} + \sqrt{E - 2\tilde{\omega}_p}}{\sqrt{E} - \sqrt{E - 2\tilde{\omega}_p}} \tag{11}$$

where N_i is the density of electrons in the ith shell. Applying the other procedure of the LPA to equation (11), we find

$$\langle S_i(E)\rangle = \frac{2\pi N_i}{E} \int \ln \frac{\sqrt{E} + \sqrt{E - 2\tilde{\omega}_p(r)}}{\sqrt{E} - \sqrt{E - 2\tilde{\omega}_p(r)}} 4\pi r^2 n_i(r)\, dr \Big/ \int 4\pi r^2 n_i(r)\, dr \tag{12}$$

where $\tilde{\omega}_p(r) = (\omega_{pi}^2(r) + \omega_i^2)^{1/2}$, $\omega_{pi}^2(r) = 4\pi n_i(r)$ and $n_i(r)$ is the electron density of the ith inner shell at a radial distance r from the nucleus. The integrations in (12) are carried out in the restricted region of r where $E > 2\tilde{\omega}_p(r)$.

4. Results and discussion

Parameters used in calculations of the dielectric function for III–V compound semiconductors are listed in table 1.

Figure 1 is the comparison of the results of measurements of Festenberg (1969) on $\varepsilon_1(0, \omega)$, $\varepsilon_2(0, \omega)$ and $\mathrm{Im}(-1/\varepsilon(0, \omega))$ for the III–IV compound GaSb with those calculated from the model used in this work. This figure shows that the model used in this work appropriately describes the sharp structures in ε_1 and ε_2 associated with the valence to conduction band transitions in the spectral region below about 8 to 10 eV, the collective plasma oscillations of valence electrons around the sharp maxima in the loss function, and the d band excitations in the loss function.

Figure 2 shows a representation of the loss function versus the energy transfer ω for several values of the momentum transfer k for InSb. One sees that when k is small, the loss function has a prominent maximum at $\omega \sim$ 13–15 eV. This maximum corresponds

Table 1. Parameters used in calculations of dielectric function for III–V compounds.

Compound	Parameter	$i = 1$	$i = 2$	$i = 3$	$i = 4$	$i = 5$
GaSb	A_i	0.0456768	0.0341755	0.1376877	0.0256316	0.0049292
	γ_i	0.0485294	0.0352941	0.1724265	0.1033088	0.1158088
	ω_i	0.0797794	0.1279412	0.1783088	0.2503676	0.78125
GaP	A_i	0.0358254	0.1768307	0.1309006	0.0087267	0.0013779
	γ_i	0.0264706	0.0775735	0.3382353	0.0569853	0.03125
	ω_i	0.1327206	0.1841912	0.2481618	0.3694853	0.7702206
GaAs	A_i	0.0580631	0.0267667	0.0835944	0.1338334	0.0185308
	γ_i	0.0452206	0.0547794	0.0518382	0.1930147	0.1819853
	ω_i	0.10625	0.1305147	0.1672794	0.2481618	0.7702206
InAs	A_i	0.0544521	0.0905307	0.1165875	0.0233843	0.0267249
	γ_i	0.0345588	0.0790441	0.2761029	0.0768382	0.2040441
	ω_i	0.0849265	0.1525735	0.2216912	0.2334559	0.7408088
InSb	A_i	0.0440140	0.0970496	0.0311652	0.0385464	0.0177696
	γ_i	0.0452206	0.1599265	0.0305147	0.1305147	0.1783088
	ω_i	0.0680147	0.1194853	0.1341912	0.2209559	0.7194853

to the possibility of plasmon excitation in the system. Note that the plasmon resonance is Landau damped by single-particle excitation and therefore is rather broad. As k increases, the plasma resonance broadens even further, and finally, for very large k, the Bethe ridge feature emerges. That is, the most probable excitation corresponds to the one in which free electron energy–momentum relation persists (Ritchie *et al* 1975).

In figure 3 we plot the (k–ω) plane in which the surface is proportional to the height of the energy loss function of GaP. The density of the shading represents the height of the surface. The valence band is plotted according to the five sub-bands with eigen-frequencies, oscillator strengths, and damping widths listed in table 1. Because of the correlation of electrons in the valence band, the contribution to the energy loss function from these sub-bands overlaps in the region of small k. The inner shells are plotted in accordance with the LPA where the damping constant $\gamma \rightarrow 0$. The broken curve shows the energy–momentum conservation relation corresponding to the minimum electron

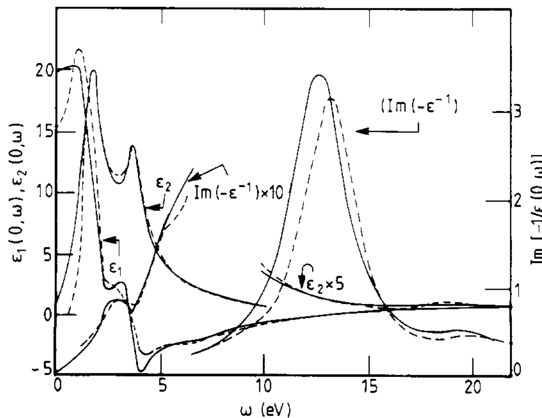

Figure 1. A comparison of experimental (broken curves) (Festenberg 1969) and theoretical (full curves) results on $\varepsilon_1(0, \omega)$, $\varepsilon_2(0, \omega)$ and $\mathrm{Im}(-1/\varepsilon(0, \omega))$ for GaSb.

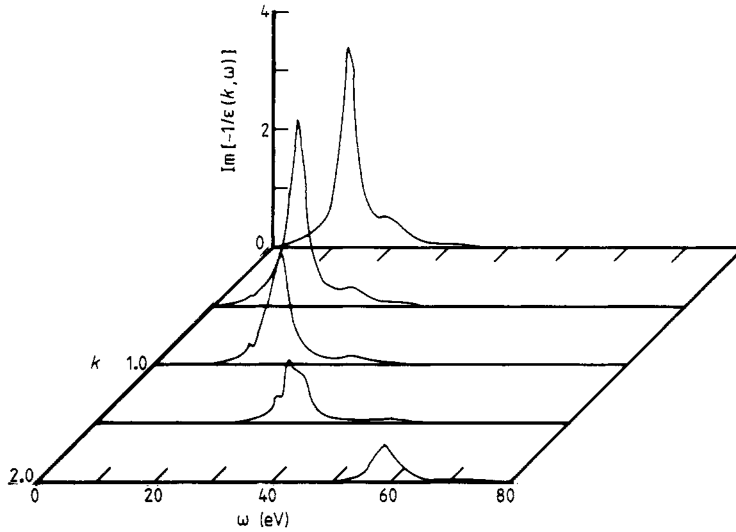

Figure 2. Energy loss function of InSb as a function of energy transfer ω, for several values of momentum transfer k.

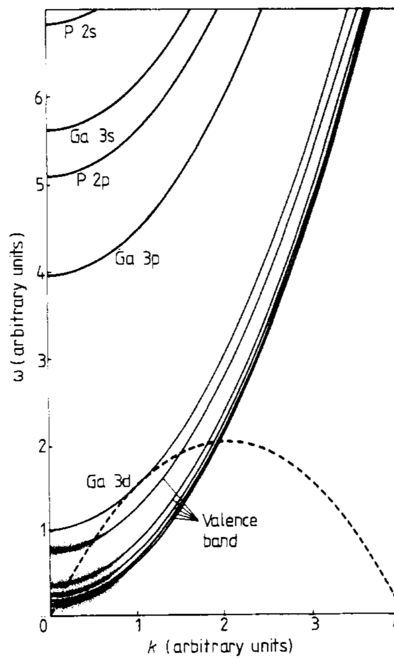

Figure 3. A representation of the $\mathrm{Im}(-1/\varepsilon(k, \omega))$ surface in the $(k - \omega)$ plane for GaP. The density of shading indicates roughly the height of the surface. The broken curve is a plot of $(2E)^{1/2}k - k^2/2$, where $E = 2\omega_i$ and i is $\mathrm{Ga_{3d}}$.

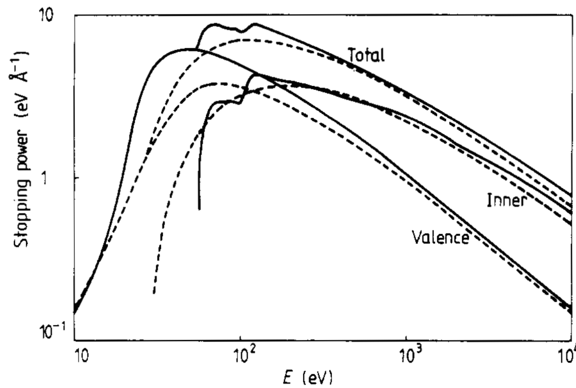

Figure 4. A plot of the stopping power for electrons against electron energy in GaAs. The full curves are the results of this work. The results of Ashley *et al* (1976) (broken curves) are included for comparison.

energy determined by $E - 2\bar{\omega}_p \geq 0$, where we plot $\bar{\omega}_p = \omega_i$ and i = Ga 3d. The intersection of this curve and the corresponding excitation spectrum exists at $k = \sqrt{\omega_i}$. In the case of space varying local-plasma frequency, $\bar{\omega}_p(r)$, determined by equation (10), the intersection occurs at $k = \sqrt{\bar{\omega}_p(r)}$.

Figure 4 shows the stopping power of GaAs as contributed by the valence band and inner shells as a function of electron energy. The corresponding results calculated by Ashley *et al* (1976) are plotted for comparison. The small structures appeared in the contribution from inner shells of the present work are due to the variation in electron density distribution, $4\pi r^2 n(r)$, and the difference in threshold energy for various shells. The contributions to the stopping power of GaAs from individual inner shells are plotted

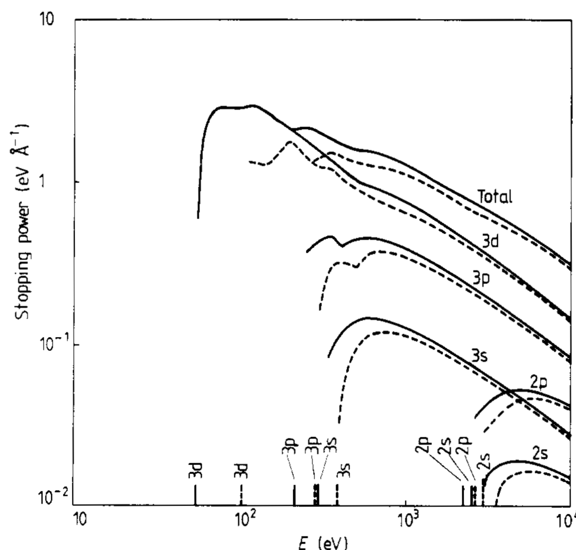

Figure 5. A plot of the stopping power for the individual inner shells of Ga (——) and As (– – –) against electron energy. The intercepts of the vertical lines on the horizontal axis indicate the corresponding threshold energies for such shells.

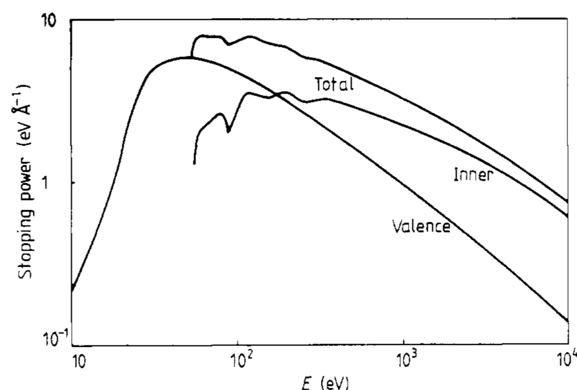

Figure 6. A plot of the stopping power for electrons against electron energy in InAs.

in figure 5. The corresponding threshold energies for such shells are labelled by the intercepts of the vertical lines with the horizontal axis. Finally, we plot figure 6 the stopping power of InAs for electrons in the energy region below 10 keV. For higher energy electrons, the stopping power may be calculated based on the Bethe theory.

5. Conclusion

Semiconducting III–V compounds are the important materials used for many applications. The stopping powers of these materials are required in the physical analyses involved in such applications. In this paper, we have presented model calculations of the stopping powers of these materials for electrons in the difficult energy region below 10 keV. An extended Drude model was employed to represent the valence band electrons in the compounds. Parameters used in this model were determined from experimental information on the energy loss measurements. Based on the local plasma approximation, quite reasonable approximate descriptions of the response of inner shell electrons are obtained. This approximation was incorporated with the electron density distribution calculated using the Hartree–Slater method to find the contribution to the stopping power from inner shells. Combining results from these two treatments, we obtained stopping powers of III–V compounds. These results should be useful for further applications.

Acknowledgment

Computing assistance from Mr L W Chen is much appreciated.

References

Ashley J C, Tung C J, Ritchie R H and Anderson V E 1976 *Rome Air Development Center Report RADC-TR-76-350*
Berger M J and Seltzer S M 1982 *National Bureau of Standards Report NBSIR 82-2550A*
Chou W K and Powers D 1972 *Phys. Lett.* **40A** 23

Fano U 1963 *Ann. Rev. Nucl. Sci.* **13** 1
Festenberg C V 1969 *Z. Phys.* **227** 453
Herman F and Skillman S 1963 *Atomic Structure Calculations* (New York: Prentice-Hall)
Lindhard J and Scharff M 1953 *K. Dan. Vidensk. Selsk. Mat. Fys. Medd.* **27** 1
Raether H 1980 *Springer Tracts in Modern Physics* **88** 48
Ritchie R H, Tung C J, Anderson V E and Ashley J C 1975 *Radiat. Res.* **64** 181
Tung C J, Ashley J C and Ritchie R H 1979 *Surf. Sci.* **81** 427
Tung C J and Lin C 1984 *Radiat. Effects* **80** 261
Tung C J and Ritchie R H 1977 *Phys. Rev.* B **16** 4302
Tung C J and Watt D E 1985 *Radiat. Effects* **90** 177
Willardson R K and Beer A C 1967 *Semiconductors and Semimetals* vol. I, II, and III (New York: Academic)
Ziegler J F 1980 *Handbook of Stopping Cross Sections For Energetic Ions in All Elements* vol 5 (New York: Pergamon)